Draft

TURBULENCE AND WAKE EFFECTS IN TIDAL STREAM TURBINE ARRAYS

Martin Nuernberg
Department of Naval Architecture, Ocean & Marine Engineering, University of Strathclyde, Glasgow, G4 0LZ, United Kingdom
Email: martin.nuernberg@strath.ac.uk

Longbin Tao
Department of Naval Architecture, Ocean & Marine Engineering, University of Strathclyde, Glasgow, G4 0LZ, United Kingdom
Email: longbin.tao@strath.ac.uk

ABSTRACT

Electricity generation from tidal current can provide a reliable and predictable addition to a reduced carbon energy sector in the future. Following the deployment of the first multi-turbine array, significant cost reduction can be achieved by moving beyond demonstrator projects to large scale tidal turbine arrays. The interactions between multiple turbines installed in close proximity can affect the total electricity generation and thus require knowledge of the resulting flow field within and downstream of the array.

Results are presented for experimental and numerical studies investigating the flow field characteristics in terms of velocity deficit and turbulence intensity in a staggered tidal turbine array section. Multiple configuration with varying longitudinal and transverse spacing between devices in a three-turbine array are tested.

Comparison between numerical and experimental flow characteristics shows that open source numerical models with dynamic mesh features achieve good agreement and can be used for the investigation of array wake effects. The standard $k - \omega$ SST shows good agreement with experiments at reduced computational efficiency compared to higher order turbulence models (RSM). The importance of mixing with ambient flow is highlighted by identifying areas of significantly reduced velocity recovery within closely spaced arrays where ambient flow does not penetrate between adjacent wakes.

INTRODUCTION

Reducing greenhouse gas emissions and the share of traditional carbon based, non-renewable energy sources in the large scale generation of electricity has led to rapid increases in the use of renewable energy sources in the last two decades.

The main drivers for the continued decarbonisation of the global energy market are renewable energy sources with wind and solar energy accounting for the largest proportion in growth of renewable energy with an average annual growth prediction of 6% and 8% respectively between 2012-2040 [1]. This development is accelerated by increased competitiveness as these sectors mature and significant reductions in cost of energy are seen [2]. Offshore wind farms have been installed gradually further offshore and reaching deeper waters with the next anticipated development being floating wind turbines in water depths beyond 40 - 60 metres, however complex interactions between mooring, floater and wind turbine dynamics have to be overcome before industrial deployment will take off.

In addition to the vast resource of offshore wind, the kinetic energy present in ocean and coastal currents can be harnessed in similar ways and provide an estimated resource in the UK that is estimated account for 10% to 15% of the total electricity generation [3, 4]. While there are a variety of prototypes in development, first commercial installations have all used horizontal axis tidal stream turbines as the preferred method of electricity generation. Following the first full scale commercial turbine generating electricity to a national grid in 2008 [5], the MeyGen array Phase 1A development, dedicated to test and monitor deployment and initial operational phases is set to be the first of a number of phases for further improvement and evaluation of deployment, foundations and turbine technology to reduce the cost of energy generation, while gradually increasing the capacity of the array towards almost 400MW in the long term [6].

For full commercialisation and continued and accelerated large scale deployment which is anticipated beyond 2020 [7], further reductions in costs, risk and complexity of offshore installations are vital. Though there are many similarities with energy extraction from large scale wind farms, significant challenges are present in the design, construction, operation and maintenance of large scale tidal farms. These include operation in bounded flows and across a significant proportion of the sheared ambient velocity profile as well as interactions between multiple turbines operating in close proximity leading to interactions of the resulting wakes within a tidal turbine array.

While the overall resource potential and extractable power was investigated using large scale one or two dimensional hydrodynamic modelling and analytical models that include the energy extraction of idealised single and multiple turbine arrangements [8-11], assessment of specific turbine performance in tidal currents uses a combination of experiments and numerical methods based on blade element momentum theory and increasingly applying RANS and LES computational

fluid dynamics modelling for combined performance, wake and array studies.

Experimental wake characterisation of single and multiple tidal turbine devices have been presented previously [12-14] utilising actuator disks and scaled three-bladed rotors respectively. Trends in velocity recovery and decay of turbulence have been similar across different experiments, generally reaching a velocity deficit of about 10% about 20 diameters (D) downstream of the turbines. Differences in wake characteristics are less pronounced with increasing downstream distance showing that, for single devices, ambient flow has large influence on the far wake characteristics while the near wake is dominated by device specific features.

Numerical simulations ranging from simplified blade element method [15] to fully resolved CFD calculations [16], have been used previously to investigate and optimise the performance of tidal turbine devices and blade sections. Numerical wake modelling by Liu, Lin [17] showed that best agreement of wake characteristics in the near and far wake was achieved by using fully resolved turbines and sliding mesh interfaces as compared to actuator disk modelling of turbine and moving reference frame to account for rotor rotation.

Experimental array studies have investigated the wake characteristics within tidal turbine arrays by means of multiple actuator disks [18] and small three bladed rotors [19, 20]. Wake velocity and turbulence statistics are presented from pointwise ADV and LDV measurements throughout the wake region and show similar trends in velocity recovery up to 20D downstream. Reductions in performance by up to 50% of a turbine operating within the wake of an upstream turbine have been shown for two axially aligned turbines [20]. Comparison of turbulence characteristics between actuator disks and small bladed rotors by Tedds et al. [14] showed over prediction of turbulent kinetic energy decay up to 9D downstream when applying simplified methods to model tidal turbine devices.

Myers, Bahaj [18] and Stallard et al. [19] observed an optimum lateral distance of 1.5D that gave rise to flow acceleration between two adjacent turbines, hence increasing the available energy to downstream devices. Staggered array configurations with three rows of turbines (Figure 1) have been investigated previously [21] and it was found that longitudinal spacing affects the wake recovery downstream of an array less than the transverse spacing of turbines.

Numerical simulations of tidal stream turbine arrays using actuator disks using an adaptive dynamic mesh by [22, 23] have shown good agreement with experiments, however require the use of empirical source terms to account for turbine specific flow features that improve agreement. Fully resolved simulations of in-line [17] and staggered array formations [24] have shown sliding mesh interfaces to result in good agreement with experiments.

This paper presents the wake characteristics of a single turbine and within a small array configuration of 4 turbines across a number of different lateral and longitudinal layout configurations. The numerical model is compared to experimentally obtained measurements and further investigation of the wake recovery with two different ambient turbulence intensities, turbulence closure models using a single turbine configuration. Further insight to the flow field characteristics of tidal turbine arrays are presented.

EXPERIMENTAL FACILITY AND MODEL

The experiments were conducted in the large Circulating-Water-Channel (CWC) at Shanghai Jiao Tong University, Shanghai, China which allows for testing in current velocities ranging from 0.2 m/s to 3.0 m/s with turbulence intensity of 2%. For the results presented here, the Reynolds number based on the diameter is 1.23×10^5 and has exceeded the threshold of 4.8×10^4 for mean velocity statistics as determined by Chamorro, Arndt [25]. The arrangement and naming of turbine arrays is shown in Figure 1, where array names for analysis of the results are provided according to the longitudinal and transverse spacing as L(a3)T(b1). Figure 2 shows the configuration with a3=5D and b1=1.5D in the test section of the CWC, thus the array is named L5T15. For all tests the maximum water depth of 1.6m was used, necessary to run the experimental facility.

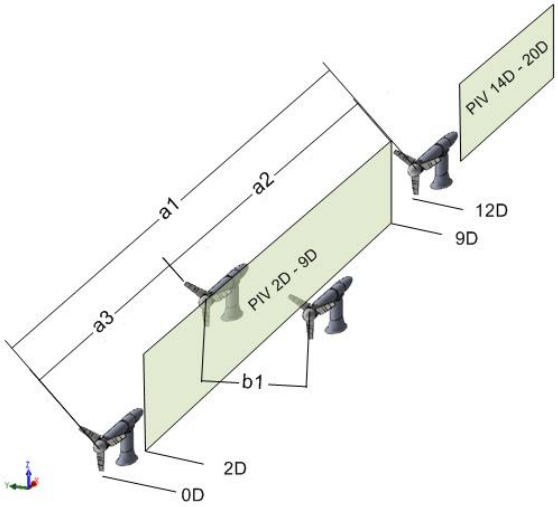

Figure 1 - Array Configuration and Measurements. Second Row Turbines Denoted "Far" (Left) and "Near" (Right).

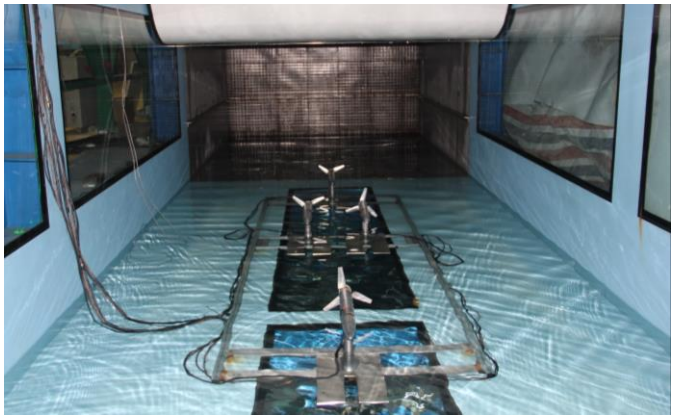

Figure 2 – Arrangement of Turbines in CWC (L5T15)

Two LaVision Imager ProX11M CCD cameras were used for PIV measurements, taken at 6 specific positions along the array centre line from 2D to 20D, with the laser sheet being projected from below the test section through a glass window and the cameras located on the side of the CWC. Thus velocity and turbulence where measured using the in-stream and vertical velocity component.

The four identical, bottom supported tidal turbine models have a rotor diameter of D = 0.28m and blades based on the NREL S814 blade section corresponding to a 1:70th scaled tidal turbine mode. A CAD drawing showing assembled design is given in Figure 3. Further details of the experiment characteristics and repeatability of measurements can be found in [21, 24].

Figure 3 - CAD Model of Scaled Turbine with Support Plate

NUMERICAL MODELLING

Fully resolved three dimensional simulations are performed in the OpenFOAM software package using the dynamic arbitrary mesh interface (AMI) to account for the rotation of the tidal turbine rotor according the rotational rates used in the experiment with a tip speed ratio (TSR) of 4, corresponding to the optimum power coefficient of the blade design as shown in [26].

The ambient flow conditions, turbine arrangement and test domain of the CWC are shown Figure 4. The domain extends from -5D upstream of the first rotor to 22D downstream, vertically there is a tip-free surface distance of 4D and the seabed to turbine tip clearance is 0.75D. The CWC free surface is not accounted for, hence top, bottom and the sides of the tank are modelled as walls. A further numerical simulation has been performed to investigate the wake recovery in 10% ambient turbulence.

The single turbine and array simulations were run in parallel on 32 processing cores using the PimpleDyMFoam solver with k-ω SST (SST) and Reynolds stress (RSM) turbulence closure model from the OpenFOAM library to a minimum simulation time of 30 seconds to ensure the flow travelled through the entire numerical domain.

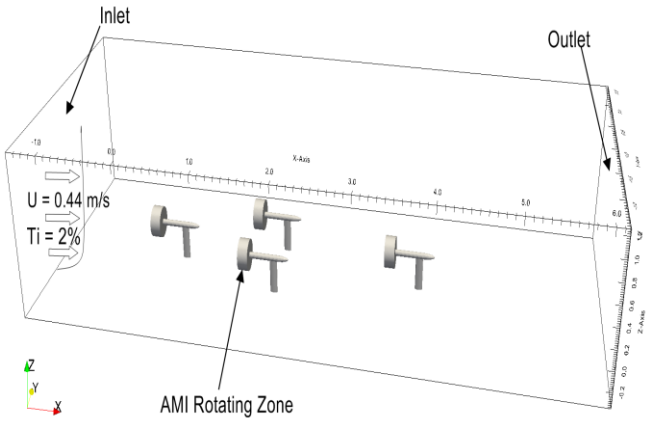

Figure 4 – Ambient Flow, Arrangement and Extent of Numerical Domain

Table 1 - GCI for Thrust (C_T) and Power Coefficient (C_P)

	Coefficient	
Mesh	**C_T**	**C_P**
Fine ($2.9x10^6$ Cells)	0.709	0.353
Medium ($8.2x10^5$ Cells)	0.698	0.336
Coarse ($3.4x10^5$ Cells)	0.704	0.341
Extr.(Fine)	0.711	0.342
GCI (%, Med)	2.9	1.57
GCI (%, Fine)	2.5	3.12

Depending on experiment configuration and number of turbines being tested, the mesh size varies from 700,000 up to 4.5 million. Numerical convergence was evaluated using the grid convergence index (GCI) for power and thrust coefficients as shown in Table 1. The mesh convergence study was performed on a single turbine using automated mesh generation with region specific refinement levels in snappyHexMesh.

The resolution of blade scale flow was validated using the pressure coefficient and compared to experiments conducted by Janiszewska, Ramsay [27] at angle of attack of 8.1 degree shown in Figure 5. Bearing in mind that these experiments where conducted at steady inflow conditions with a constant blade profile along the blade radius, the transient numerical results from the experimental study presented here are judged as agreeing well with the published data.

In-line velocity characteristics shown in Figure 6 at the turbine rotor centre height were compared across three different mesh resolutions and showed little differences between the medium and fine configuration, thus to reduce the computational resource requirements, the medium resolution was shown for all further simulations. Further details and discussion of the mesh generation and validation are presented in [24].

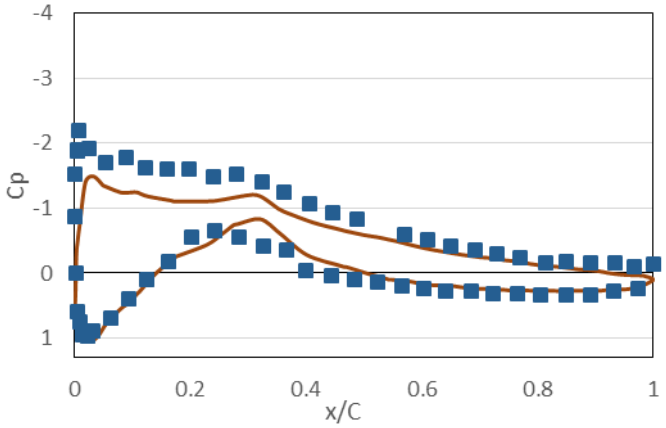

Figure 5 – Pressure Coefficient (Cp) Comparison at Blade Section r/R=0.67 with Experiments [27] at Re=750,000 (Box) and Simulations (Line)

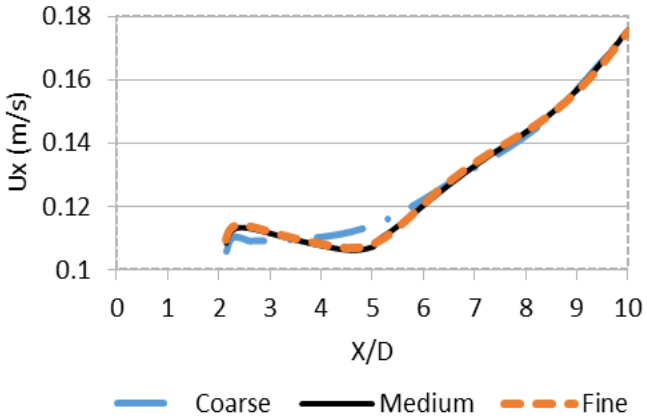

Figure 6 - Mesh Convergence For In-line Velocity Component at 0.25m/s Ambient Flow

RESULTS AND DISCUSSION

The wake recovery of a single turbine is presented in Figure 7 for the experiments and numerical simulations including a comparison to numerical simulations at higher ambient turbulence intensity of 10%.

The far wake velocity recovery reaches a deficit of approximately 13% at 20D downstream of the isolated turbine. The most pronounced differences occur in the immediate near wake downstream of the nacelle body, where the SST model shows increasing velocity deficit closer to the nacelle than observed in experiments and with a higher peak deficit. For increased ambient turbulence, there is no increase in velocity deficit immediately downstream of the nacelle where the shear layers reach the rotor centre line.

Comparison between different turbulence closure models shows that SST and RSM agree well with the experimentally obtained wake recovery for most of the measurement domain. Differences in the very near wake between 2D-4D are due to the interaction of slow moving wakes downstream of the rotor blades and accelerated flow around the nacelle body as shown in Figure 8 being captured differently by each model and occurring closer to the nacelle in the SST model than in the experiment. The increase in velocity deficit was observed between 4D and 5D in experiments while numerical simulation showed this between 2D and 4D.

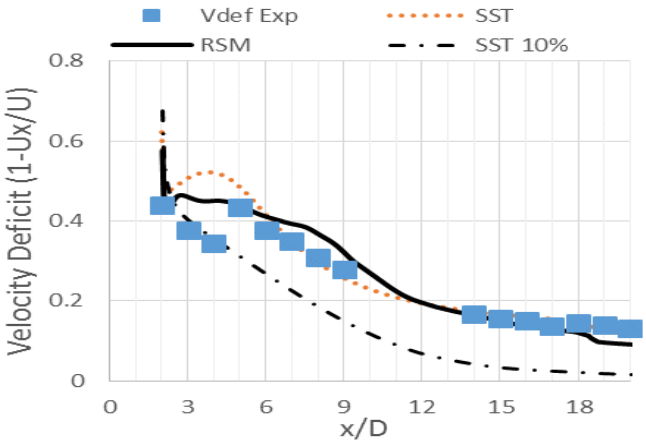

Figure 7 - Comparison of Experimental Wake Velocity Deficit with Numerical SST and RSM Turbulence Closure at 2% Ambient Turbulence (SST) and SST Turbulence Closure at High Ambient Turbulence Intensity of 10% (SST 10%)

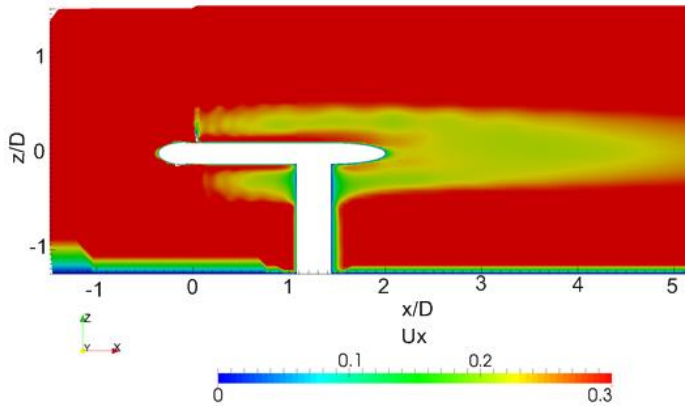

Figure 8 – In-Stream Velocity Component Around the Tidal Turbine Support Structure Showing Waken Expanding Towards the Rotor Centre Line

The wake recovery in array for Array L3T15 is shown in Figure 9 with the comparison of experimentally obtained and numerical simulation. The agreement between the velocity deficit between experiments and numerical simulation is very good across the measurement domain with differences being most significant in areas with high velocity shear in close proximity to the turbine nacelle. Small differences are seen between 3D to 5D where flow recovery is accelerated in the experiments and an increase in velocity deficit is observed from the numerical simulations. In addition to this, during the experiments visual access to the array centre line was impacted by the turbine models being located on the second row of the

array between 3D – 5D. Little recovery is observed for close transverse and longitudinal spacing between 5D and 10D in the experiments and similar trends are shown in the numerical simulations where this large volume of slow moving fluid was identified (Figure 10).

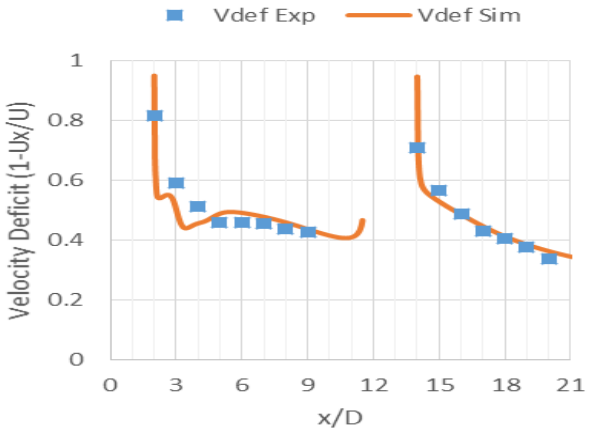

Figure 9 - Wake Velocity Recovery of L3T15 Array for Experiments (Box) and Simulations (Line)

The evolution of the centre line velocity deficit downstream of the second row turbines until just upstream of the third row turbine is shown in Figure 10. The close transverse spacing of L3T15 and L5T15 show increasing velocity deficits up to 2D downstream of the respective middle row turbines and reduced velocity recovery further downstream as compared to the wide transverse spacing of L3T3 and L5T3. Initially the recovery is accelerated for the L5T15 array between the two rotors located off the array centreline at 5D, indicating the ambient flow being directed towards the array centre. Further downstream the velocity deficits increase due to the influence of the second row turbines. The wide transverse cases show steadier wake recovery, although small increases are seen for L5T3 between 7D - 10D. Between 2D and 0.5D upstream of the last row turbine the velocity deficit increases for all cases ranging from 5% increase for the closely spaced arrays to 10% for wide transverse separation of the middle row turbines. 1D upstream of the downstream turbine inflow velocity deficit is 10% lower for the L5T3 case compared to L5T15 while the difference for the L3T15 to L3T3 array is about 6%.

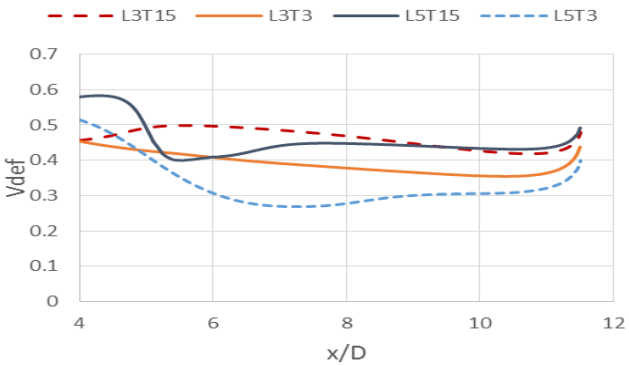

Figure 10 – Comparison of Numerical Wake Recovery at the Array Centre Line from Numerical Simulations.

The wake mixing within and downstream of the array configurations is shown in Figure 11 for further investigation of the transverse distribution of Reynolds stresses in the xy plane, comparing the Reynolds stress field within the array among four different array configurations with minimum and maximum transverse spacing for both longitudinal configurations.

The most significant observation is that with close transverse and longitudinal spacing for the L3T15 array in (a), very little mixing occurs at the centre part of the array downstream of the second row turbines. In comparison with L5T15 in (c), the flow re-energisation at the centreline is greatly reduced and mixing occurs mostly with the ambient flow either side of the array section. This corresponds to the existence of a large volume of very slow moving fluid as identified in experiments and numerical simulations previously where little velocity recovery occurs and shows the beneficial effects of longitudinal spacing increasing the wake mixing within the array. For both close transverse spacing arrays the mixing downstream of the array section shows similar characteristics with an increase in mixing around the turbine and a more diffused field of increased Reynolds stresses further downstream.

With wide transverse spacing, mixing can be observed on each individual wake as well as downstream of the array section. The ambient flow between adjacent wakes can clearly be seen as a small volume where little mixing occurs. This persists through the entire array section. From the obtained data it can also be seen that the wakes of the two outer turbines of the middle row are diverted around the centre wake of the downstream turbine. Increased mixing for a longer distance is observed downstream of the array section.

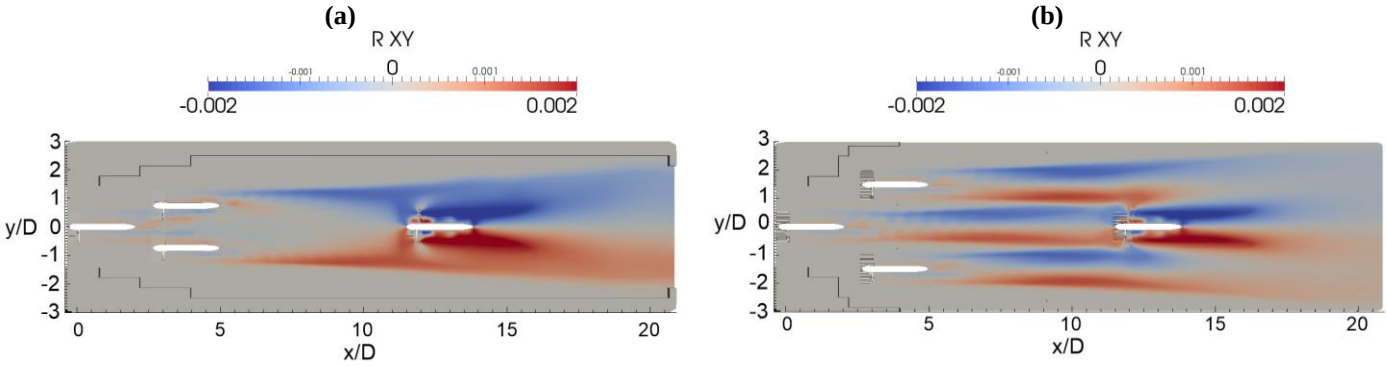

Figure 11 - Comparison of Reynolds Stresses in (*xy*) Plane Between (a) L3T15 and (b) L3T3 Array Configuration

The Q-criterion is used to visualise vortices and shows the evolution of these downstream of the rotor. With low ambient turbulence, the breakdown of vortices shed of the turbine blades is delayed as can be seen in Figure 12 (a) and (b), showing a comparison between a single turbine at two different ambient turbulence levels (2% and 10%) in the near wake up to 6D. The upstream and the downstream array turbine vortices are shown for L3T15 in (c) and L5T3 in (d). The spacing between vortices increases around the area where the vertical support interferes and vortices begin to break down. The wake contracts between the second row turbines in L5T3 and where the shear layer starts expanding, about 2D downstream of the two rotors located at 5D, the vortices of the outer wakes break down and wake expansion is observed for the outer wakes.

The vortices shed by the Far and Near turbine are significantly affected for L3T15 and break down within a distance of 1D downstream of the rotor due to being located in the turbulent wake of the upstream turbine. The downstream turbine shows the vortices to break down immediately downstream of the rotor due to the highly turbulent inflow. Wake expansion of the downstream turbine is more significant immediately downstream of the vortex break-down for the downstream turbine.

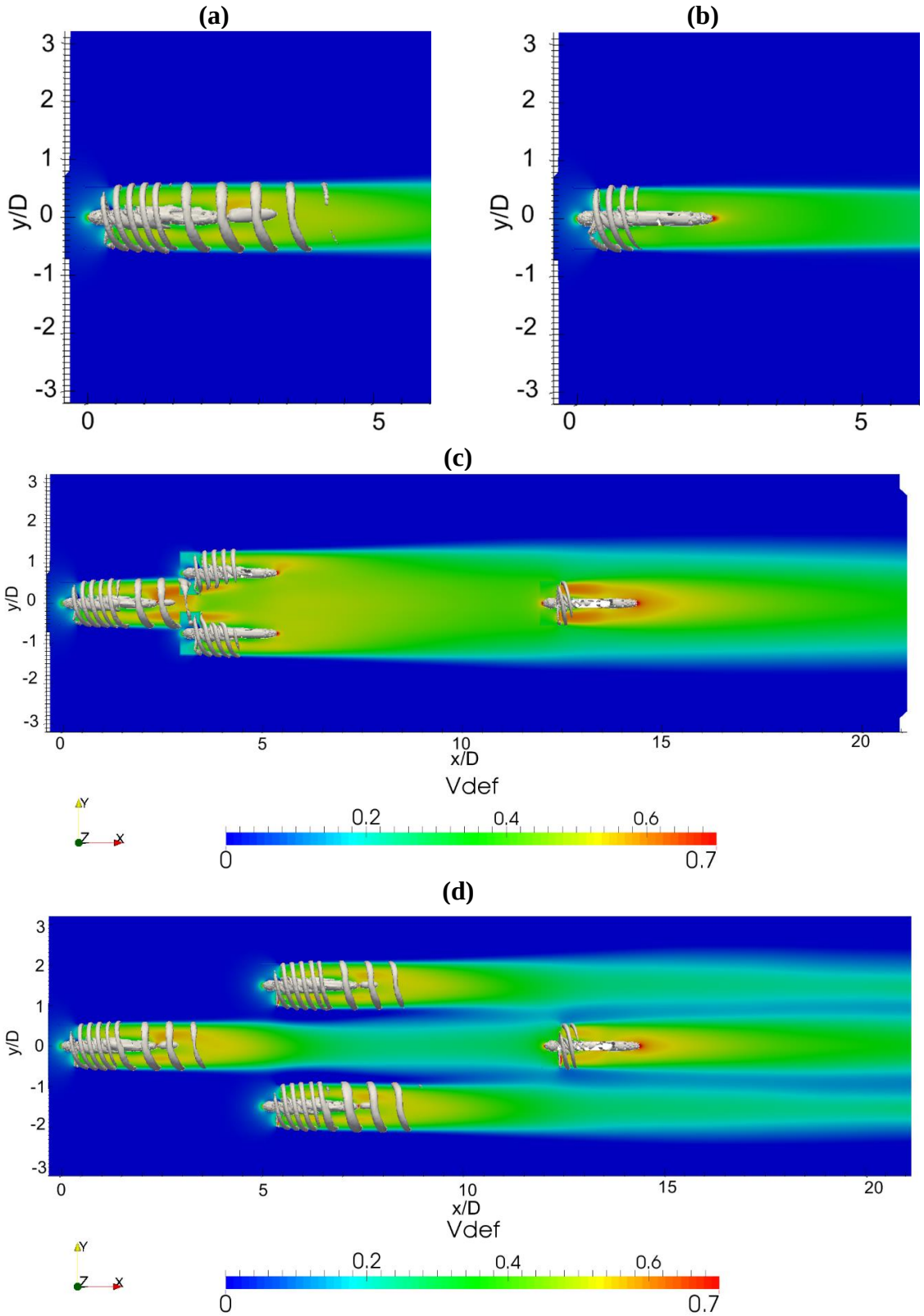

Figure 12 - Velocity Deficit and Q-criterion (Q=2) for Propagation of Vortices Around the Turbine Support Structure for (a) Single 2% (b) Single 10% (c) L3T15 and (d) L5T3 Array.

CONCLUSION

Wake velocity and turbulence characteristics have been recorded for a range of scale mode tidal turbine array configurations tested in a circulating water channel and fully resolved three dimensional numerical simulations with dynamic mesh features performed in OpenFOAM.

Agreement between single turbine and array wake characteristics was shown to be good between the conducted experiments and numerical simulations. Some areas of the wake, especially near the turbine nacelle showed large differences where visual access to the array centre line for PIV measurements was affected during the experiments.

RSM and k – ω SST turbulence closure models showed similar predictions of wake velocity deficit. The RSM model performed better closer to the turbine, where the effect of rotating flows and increased turbulence are significant.

Increased ambient turbulence intensity significantly reduced wake recovery and led to immediate reduction of the velocity deficit in the near wake of the turbine. For low ambient turbulence, the acceleration around the turbine nacelle resulted in an initial decrease of velocity deficit followed by an increase where the upper and lower layer of the wake reach the rotor centreline. The evolution of vortices was strongly reduced in high ambient turbulence intensity environment.

Array flow field characteristics showed that mixing with ambient flow in wide transverse spacing led to improved velocity recovery within the array. For close longitudinal and transverse spacing, a large volume of slow moving fluid was trapped at the array centre line where little to no reduction in velocity deficit occurred.

Due to the increased mixing with ambient flow and the turbulent wake of the second row turbines either side of the downstream turbine, the wake recovery of the downstream turbine was less affected by the positioning of the second row turbines and showed accelerated wake recovery at the array centre line.

ACKNOWLEDGMENTS

The authors gratefully acknowledge the support received in conducting this experiment by the School of Naval Architecture, Ocean and Civil Engineering at Shanghai Jiao Tong University and the British Council (China) under the “Sino-UK Higher Education Research Partnership” as well as LaVision for providing support and software for the PIV analysis. The numerical work made use of the facilities of N8 HPC provided and funded by the N8 consortium and EPSRC (Grant No.EP/K000225/1). The center is co-ordinated by the Universities of Leeds and Manchester.

REFERENCES

1. EIA, *International Energy Outlook 2016*. 2016, U.S. Energy Information Administration.
2. ORE CATAPULT, *Cost Reduction Monitoring Framework 2016*. 2016, Offshore Renewable Energy Catapult.
3. Carbon Trust, *Accelerating Marine Energy*. 2011.
4. Carbon Trust, *UK Tidal Current Resource & Economics* 2011.
5. Marine Current Turbines. *World's first commercial-scale tidal power system feeds electricity to the National Grid*. 2008 04/06/2014]; Available from: http://www.marineturbines.com/3/news/article/10/worlds_first_commercial_scale_tidal_power_system_feeds_electricity_to_the_national_grid .
6. Atlantis Resources Ltd. *Meygen Project Development & Operation*. 2017 [cited 2017 31/05/17]; Available from: https://www.atlantisresourcesltd.com/projects/meygen/.
7. DECC, *Renewable Energy Roadmap 2011*. 2011, Department of Energy and Climate Change, London, UK.
8. Garrett, C. and P. Cummins, *The efficiency of a turbine in a tidal channel.* Journal of Fluid Mechanics, 2007. **588**: p. 243-251.
9. Ahmadian, R. and R.A. Falconer, *Assessment of array shape of tidal stream turbines on hydro-environmental impacts and power output.* Renewable Energy, 2012. **44**: p. 318-327.
10. Funke, S.W., P.E. Farrell, and M.D. Piggott, *Tidal turbine array optimisation using the adjoint approach.* Renewable Energy, 2014. **63**: p. 658-673.
11. Vennell, R., *Estimating the power potential of tidal currents and the impact of power extraction on flow speeds.* Renewable Energy, 2011. **36**(12): p. 3558-3565.
12. Myers, L.E. and A.S. Bahaj, *Experimental analysis of the flow field around horizontal axis tidal turbines by use of scale mesh disk rotor simulators.* Ocean Engineering, 2010. **37**(2-3): p. 218-227.
13. Mycek, P., et al., *Experimental study of the turbulence intensity effects on marine current turbines behaviour. Part I: One single turbine.* Renewable Energy, 2014. **66**(0): p. 729-746.
14. Tedds, S.C., I. Owen, and R.J. Poole, *Near-wake characteristics of a model horizontal axis tidal stream turbine.* Renewable Energy, 2014. **63**(0): p. 222-235.
15. Bahaj, A.S., W.M.J. Batten, and G. McCann, *Experimental verifications of numerical predictions for the hydrodynamic performance of horizontal axis marine current turbines.* Renewable Energy, 2007. **32**(15): p. 2479-2490.
16. McNaughton, J., et al., *A simple sliding-mesh interface procedure and its application to the CFD simulation of a tidal-stream turbine.* International Journal for Numerical Methods in Fluids, 2014. **74**(4): p. 250-269.

17. Liu, J., H. Lin, and S.R. Purimitla, *Wake field studies of tidal current turbines with different numerical methods.* Ocean Engineering, 2016. **117**: p. 383-397.
18. Myers, L.E. and A.S. Bahaj, *An experimental investigation simulating flow effects in first generation marine current energy converter arrays.* Renewable Energy, 2012. **37**(1): p. 28-36.
19. Stallard, T., et al., *Interactions between tidal turbine wakes: experimental study of a group of three-bladed rotors.* Philos Trans A Math Phys Eng Sci, 2013. **371**(1985): p. 20120159.
20. Mycek, P., et al., *Experimental study of the turbulence intensity effects on marine current turbines behaviour. Part II: Two interacting turbines.* Renewable Energy, 2014. **68**: p. 876-892.
21. Nuernberg, M. and L. Tao, *Experimental Study of Flow Field Characteristics in Tidal Stream Turbine Arrays.* Proceedings of the International Conference on Offshore Mechanics and Arctic Engineering - OMAE, 2016(49972): p. V006T09A004.
22. Abolghasemi, M.A., et al., *Simulating tidal turbines with multi-scale mesh optimisation techniques.* Journal of Fluids and Structures, 2016. **66**: p. 69-90.
23. Shives, M. and C. Crawford, *Adapted two-equation turbulence closures for actuator disk RANS simulations of wind & tidal turbine wakes.* Renewable Energy, 2016. **92**: p. 273-292.
24. Nuernberg, M. and L. Tao, *Three dimensional tidal turbine array simulations using OpenFOAM with dynamic mesh*. Ocean Engineering, 2017.
25. Chamorro, L.P., R.E.A. Arndt, and F. Sotiropoulos, *Reynolds number dependence of turbulence statistics in the wake of wind turbines.* Wind Energy, 2012. **15**(5): p. 733-742.
26. Shi, W.C., et al., *Flow separation impacts on the hydrodynamic performance analysis of a marine current turbine using CFD.* Proceedings of the Institution of Mechanical Engineers Part a-Journal of Power and Energy, 2013. **227**(8): p. 833-846.
27. Janiszewska, J.M., et al., *Effects of grit roughness and pitch oscillations on the S814 airfoil*. 1996, National Renewable Energy Lab., Golden, CO (United States).